JPET Fast Forward. Published on November 3, 2016 as DOI: 10.1124/jpet.116.237388
This article has not been copyedited and formatted. The final version may differ from this version.

Title page

TAK-063, a novel phosphodiesterase 10A inhibitor, protects from striatal neurodegeneration and ameliorates behavioral deficits in the R6/2 mouse model of Huntington's disease

Akina Harada, Kazunori Suzuki, and Haruhide Kimura

CNS Drug Discovery Unit, Pharmaceutical Research Division, Takeda Pharmaceutical Company Limited, Fujisawa, Kanagawa, Japan

Running title page

Running Title:

Pharmacological characterization of TAK-063 in R6/2 mice

Address correspondence to:

Haruhide Kimura, Pharmaceutical Research Division, Takeda Pharmaceutical Company Limited, 26-1, Muraoka-Higashi 2-chome, Fujisawa, Kanagawa 251-8555, Japan

Phone number: (+81) 466321859

Fax number: (+81) 466294468

E-mail: haruhide.kimura@takeda.com

Number of text pages: 46

Number of tables: 1

Number of figures: 7 (including one supplemental figure)

Number of references: 60

Number of words in Abstract: 247

Number of words in Introduction: 748

Number of words in Discussion: 1352

Abbreviations:

BDNF, brain-derived neurotrophic factor

CAG, cytosine-adenine-guanine

CFC, contextual fear conditioning

CREB, cAMP response element-binding protein

HD, Huntington's disease

MSN, medium spiny neuron

PBS, phosphate buffered saline

PDE, phosphodiesterase

RM-ANOVA, repeated measures analysis of variance

RT, room temperature

TAK-063

[1-[2-fluoro-4-(1*H*-pyrazol-1-yl)phenyl]-5-methoxy-3-(1-phenyl-1*H*-pyrazol-5-yl)pyridazin-4

(1*H*)-one]

Tg, transgenic

WT, wild-type

Recommended section assignment:

Neuropharmacology

Abstract

Huntington's disease (HD) is characterized by progressive loss of striatal medium spiny neurons (MSNs) that constitute direct and indirect pathways: the indirect pathway MSNs is more vulnerable than the direct pathway MSNs. Impairment of cAMP/cGMP signaling by mutant huntingtin is hypothesized as the molecular mechanism underlying degeneration of MSNs. Phosphodiesterase 10A (PDE10A) is selectively expressed in MSNs and degrades both cAMP and cGMP; thus, PDE10A inhibition can restore impaired cAMP/cGMP signaling. Compared with other PDE10A inhibitors, a novel PDE10A inhibitor TAK-063 [1-[2-fluoro-4-(1H-pyrazol-1-yl)phenyl]-5-methoxy-3-(1-phenyl-1H-pyrazol-5-yl)pyridazin-4 (1H)-one] showed comparable activation of the indirect pathway MSNs, while it produced partial activation of the direct pathway MSNs by its faster off-rate property. Here, we report the effects of TAK-063 on striatal neurodegeneration and behavioral deficits in the R6/2 mouse model of HD. TAK-063 at 0.5 or 5 mg/kg/day was orally administrated from 4.5–5 to 12 weeks of age, and the effects of TAK-063 were characterized over this period. Repeated treatment with TAK-063 suppressed the reduction of BDNF levels, prevented striatal neurodegeneration, and suppressed increase in seizure frequency, but did not prevent the suppression of body weight gain. As for motor deficits, TAK-063 suppressed the development of clasping behavior and motor dysfunctions, including decreased motor activity in the open field, but did not improve the impairment in motor coordination on the rotarod. Regarding

cognitive functions, TAK-063 improved deficits in procedural learning, but was ineffective for deficits in contextual memory. These results suggest that TAK-063 reduces striatal neurodegeneration and ameliorates behavioral deficits in R6/2 mice.

Introduction

Huntington's disease (HD) is an autosomal dominant, inherited neurodegenerative disease associated with progressive cognitive impairment and motor symptoms such as chorea, akinesia, and dystonia (Walker, 2007; Ross and Tabrizi, 2011). HD is caused by a mutation that results in an abnormal expansion of cytosine-adenine-guanine (CAG) trinucleotide repeats beyond about 35 repeats within exon 1 of the huntingtin gene, which encodes the huntingtin protein (Walker, 2007; Frank, 2014; Ross et al., 2014). Although mutant huntingtin is expressed throughout the brain, the most prominent cell loss is of medium spiny neurons (MSNs) in the striatum (Vonsattel and DiFiglia, 1998). The MSNs constitute two distinct output pathways: the direct and indirect pathways (Graybiel, 1990; Graybiel, 2000). Particularly, indirect pathway MSNs appear to be more vulnerable to degeneration than direct pathway MSNs in patients with HD (Reiner et al., 1988; Sapp et al., 1995; Glass et al., 2000; Galvan et al., 2012). So far, multiple animal models of HD have been established (Pouladi et al., 2013). HD model mice, such as R6/2, CAG140 and YAC128 mice, are initially hyperactive and gradually become hypoactive (Lüesse et al., 2001; Menalled et al., 2003; Slow et al., 2003), suggesting the reduced output from both direct and indirect pathway MSNs. Those phenotypes might reflect the higher vulnerability of indirect pathway MSNs than direct pathway MSNs at earlier phases, although the direct evidence is limited. Interestingly, green fluorescent protein, selectively expressed in indirect pathway MSNs under Drd2 promoter

control, was reduced from early stages of disease progression in R6/2, R6/1, CAG140, and HdhQ111 mice (Crook and Housman, 2012). Those HD model mice might not completely replicate the HD pathology; however, these mice would be useful for preclinical evaluation of potential therapeutics for the treatment of HD. Impairment in cAMP signaling and its downstream cAMP response element-binding protein (CREB) signaling pathway by mutant huntingtin protein has been hypothesized to play a critical role in the neurodegeneration in HD pathology (Nucifora et al., 2001; Wyttenbach et al., 2001; Mantamadiotis et al., 2002; Gines et al., 2003; Sugars and Rubinsztein, 2003; Choi et al., 2009). Neuronal nitric oxide synthase mRNA is also decreased in the postmortem striatum of patients with HD (Norris et al., 1996), suggesting the downregulation of cGMP signaling. Thus, activation of cAMP and cGMP signaling pathways, especially in indirect pathway MSNs, could be a potential therapeutic approach for HD.

Phosphodiesterase 10A (PDE10A) is a dual-substrate PDE that hydrolyzes both cAMP and cGMP, and is highly expressed in both direct and indirect pathway MSNs (Fujishige et al, 1999; Seeger et al., 2003; Coskran et al., 2006). PDE10A inhibitors activate both types of MSNs, and previous studies suggested the indirect pathway preferential activation by PDE10A inhibitors such as papaverine, TP-10, and MP-10 (Nishi et al., 2008; Threlfell et al., 2009; Wilson et al., 2015). A selective PDE10A inhibitor TP-10 significantly increased striatal cell survival and activated CREB in the quinolinic rat model of HD (Giampà et al.,

2009). TP-10 also showed significant beneficial effects in R6/2 mice; it recovered striatal and cortical levels of phosphorylated CREB and BDNF, inhibited striatal atrophy, and showed improvement in clasping behavior, performance in rotarod, and locomotor activity (Giampà et al., 2010). TP-10 was reported to increase the corticostriatal transmission via upregulation of cGMP signaling (Padovan-Neto et al., 2015), which might also contribute to its beneficial effects in the quinolinic rat model and R6/2 mice. Thus, restoring cAMP and cGMP signaling by PDE10A inhibition may be a promising treatment approach for HD. TAK-063 [1-[2-fluoro-4-(1H-pyrazol-1-yl)phenyl]-5-methoxy-3-(1-phenyl-1H-pyrazol-5-yl)-pyridazin-4(1H)-one] is a selective and orally active PDE10A inhibitor (Kunitomo et al., 2014). Interestingly, our previous study revealed that activation pattern of MSNs by a faster off-rate PDE10A inhibitor TAK-063 was different from those by slower off-rate PDE10A inhibitors such as MP-10 and compound 1; compared to MP-10 and compound 1, TAK-063 equally activated indirect pathway MSNs, whereas it partially activated direct pathway MSNs (Suzuki et al., 2016). Considering the lower vulnerability of direct pathway MSNs than that of indirect pathway MSNs, this MSN activation pattern by TAK-063 could protect MSNs in both pathways from neurodegeneration by mutant huntingtin without unbalanced activation of these pathways.

In this study, we investigated the effects of TAK-063 on the R6/2 mouse model of HD. R6/2 mouse line is a widely used transgenic (Tg) mouse model of HD with several

phenotypes similar to that seen in patients with HD, including striatal atrophy, motor deficits, and cognitive impairments. Here, we report preclinical evidence that TAK-063 protects from striatal neurodegeneration and ameliorates behavioral deficits in R6/2 mice.

Materials and Methods

Ethics Statement. All behavioral studies were conducted by PsychoGenics Inc. (Tarrytown, NY) according to principles of the Public Health Service Policy on Humane Care and Use of Laboratory Animals, and procedures were approved by the Institutional Animal Care and Use Committee of PsychoGenics Inc. (IACUC protocol number: 179_0312). PsychoGenics Inc. achieved Association for Assessment and Accreditation of Laboratory Animal Care International accreditation (AAALAC Unit #001213).

Animals. R6/2 Tg mice carrying the N-terminal region of a mutant human huntingtin gene and wild-type (WT) mice were used in this study (Mangiarini et al., 1996). Mice were bred in the colony of PsychoGenics Inc. by crossing ovarian transplanted females on a CBA×C57BL/6 background (The Jackson Laboratory, Bar Harbor, ME) with male C57BL/6 mice. Mice were identified before weaning by real-time PCR of tail snips. CAG repeat length in mutant mice was analyzed by ABI Prism 377 DNA Sequencer (Life Technologies, Carlsbad, CA). Average CAG repeat lengths for each R6/2 mouse group were as follows:

vehicle-treated group, 123.79 ± 0.35; 0.5 mg/kg/day of TAK-063–treated group, 123.34 ± 0.48; 5 mg/kg/day of TAK-063–treated group, 123.66 ± 0.49 (mean ± SEM; n = 19–22). Mice were given 1-min handling habituation on 2 consecutive days between 19–21 days of age, and were identified by tail tattoo at 20–21 days of age and weaned at 21–22 days of age. Mice were housed in a room with light control (12-h light/12-h dark cycle with lights on at 7:00 AM). Food and water were provided *ad libitum*. Animals were checked for survival twice per day and body weighed once per week. Mice from multiple littermates were used for each treatment group (almost equally divided between sexes), and housed 4–5 mice/cage. Two WT mice of the same sex, but different littermates, were included in each cage for providing normal social stimulation.

Chemicals. TAK-063 [1-[2-fluoro-4-(1*H*-pyrazol-1-yl)phenyl]-5-methoxy-3-(1-phenyl-1*H*-pyrazol-5-yl)-pyridazin-4(1*H*)-one] was synthesized by Takeda Pharmaceutical Company Limited (Fujisawa, Japan). TAK-063 was suspended in vehicle (0.5% methylcellulose in sterile water) using an ultrasonic sonicator for 10 min and was then mixed by pipetting and inverting the tube to eliminate any precipitation. Dosing solutions were formulated daily. All formulated dosing solutions were prepared in amber glass vials. The formulated solutions were additionally stirred for at least 10 min before dosing and were stirred throughout the dosing session. Daily oral

administration of vehicle or TAK-063 at 0.5 mg/kg or 5 mg/kg with a dose volume of 10 mL/kg was started from 4.5–5 to 12 weeks of age. The drugs were administered after the completion of behavioral tests each day. No mice were dead up to 12 weeks of age.

Biochemical Analysis. At 12 weeks of age (after 8 weeks of repeated dosing and behavioral studies), mice (n = 6 in each group) were sacrificed and tissue collected 3 h after the last administration. Plasma samples of TAK-063-treated groups were also collected at the same time point. The plasma concentrations of TAK-063 at 0.5 and 5 mg/kg/day were 191.2 ± 11.0 and 1123.5 ± 32.5 ng/mL, respectively (mean ± S.E.M., n = 7). Striatal PDE10A occupancies of TAK-063 at plasma concentrations of 191.2 and 1123.5 ng/mL are estimated as 58 and 89%, respectively, in mice (Supplemental Fig. 1). The brains were rapidly removed and rinsed in ice cold saline. The striatum and cerebral cortex were then immediately dissected and frozen on dry ice. The dissected tissues were homogenized by ultrasonic sonication in 20 mL/g of lysis buffer (137 mM NaCl, 20 mM Tris-HCl pH 8.0, 1% NP40, 10% glycerol, and 1% proteinase inhibitor cocktail). The homogenates were centrifuged at 15,000 rpm for 20 min at 4°C, and the supernatants were frozen at −80°C until use. Brain-derived neurotrophic factor (BDNF) levels were determined using BDNF $E_{max}^{®}$ ImmunoAssay System kit (Promega, Madison, WI) following the manufacturer's instructions. The 96-well plates coated with anti-BDNF monoclonal antibody were incubated with a blocking buffer at room temperature

(RT) for 1 h. The frozen samples and BDNF standards were applied to the plates. The plates were incubated with shaking for 2 h at RT, followed by rinse with the washing buffer. Then, the plates were incubated with anti-BDNF polyclonal antibody for 2 h at RT, and were rinsed with the washing buffer. The plates were incubated with horseradish peroxidase-conjugated anti-IgY antibody for 1 h at RT. To produce a color reaction, the solution of peroxidase substrate and tetramethylbenzidine was added to the plates. The reaction was terminated by addition of 1 M hydrochloric acid, and then the absorbance was measured at 450 nm using a plate reader Wallac ARVO SX 1420 (PerkinElmer, Waltham, MA).

Histochemical Analysis. At 12 weeks of age (after 8 weeks of daily dosing and behavioral studies), mice (n = 4 in each group, 2 males and 2 females) were randomly selected and were anesthetized with sodium pentobarbital and transcardially perfused with saline, followed by 4% paraformaldehyde in 0.1 M phosphate buffered saline (PBS) 3 h after the last administration. The whole brain was removed and fixed overnight in 4% paraformaldehyde in 0.1 M PBS at 4°C and then transferred to a solution of 30% sucrose in 0.1 M PBS at 4°C. The brains were embedded in 7.5% sucrose containing Tissue-Tek OCT Compound (Sakura Finetek, Tokyo, Japan) and were stored at −80°C until use. Multiple coronal serial sections per animal (20 μm thick) within the coordinates of 0.86–0.50 mm rostrocaudal from bregma, were cut on a cryostat. Two sections per animal were randomly selected from the multiple

sections for the following staining. Cresyl violet (MP Biomedicals, Aurora, OH) was used to stain Nissl substance in the cytoplasm of neurons. The sections were rehydrated through graded alcohols and then stained with 0.07% acetic acid containing 0.25% aqueous solution of cresyl violet for 30 min. The sections were briefly rinsed with water, followed by dehydration in graded alcohols. The sections were cleared in xylene and were sealed by coverslips. Images of stained sections were captured at ×20 magnification by a slide scanner (NanoZoomer, Hamamatsu Photonics, Hamamatsu, Japan). To assess striatal atrophy, the bilateral striata of the sections were manually delineated according to the stereotaxic atlas of the mouse brain (Paxinos and Franklin, 2001) using NDP viewing software (Hamamatsu Photonics) by an investigator blind to the treatment groups. The defined striatal areas (mm^2) were automatically calculated by the same software. The bilateral striatal areas were averaged between two sections per animal, and further averaged over each treatment group (n = 4).

Experimental Design of Behavioral Study. All testing and assessments were performed during the animals' light cycle phase. Mice in their home cages were transferred from the rearing room to the experimental rooms and were acclimated to the experimental rooms for at least 1 h before the beginning of any experiments. At 4 weeks of age, mice were tested for rotarod and open field behaviors for validation of baseline phenotypes. Mice were balanced between four treatment groups (vehicle-treated WT mice, vehicle-treated R6/2 mice, 0.5

mg/kg/day of TAK-063–treated R6/2 mice, and 5 mg/kg of TAK-063–treated R6/2 mice) in terms of sex, body weight, CAG repeat number, and past behavioral performance. Experimenters were blind to both treatment and genotype at time of behavioral testing.

Body Weight. Mice were weighed once per week throughout the study (4–12 weeks of age).

Clasping Behavior. Clasping behavior was weekly assessed at the time body weights were measured. Mice were suspended by the tail for 30 s and observed for hind limb clasping. The percentages of mice showing full clasping behavior within 30 s were calculated at 5–12 weeks of age.

Open Field Test. The open field test was conducted in a Plexiglas square chamber (27.3×27.3×20.3 cm; Med Associates Inc., St. Albans, VT) surrounded by infrared photobeam sources. Horizontal activity (distance traveled) and vertical activity (rearing) were measured by infrared photobeam sources from consecutive beam breaks. Animals were placed in the chambers for 30 min, and total ambulatory distance and total rearing were measured. Mice were tested at 4 (baseline) and 12 weeks of age.

Rotarod Test. Rotarod test was performed over 3 consecutive days at 4 (baseline), 6, and 12

weeks of age. Mice were placed on the rotarod and the speed of rotation was gradually and uniformly increased 4 to 40 rpm over 300 s. The latency to fall off from the rotarod was recorded up to 300 s.

Procedural Water T-Maze Test. To investigate procedural learning and cognitive flexibility, procedural water T-maze test was performed using a T-shaped water maze in mice at 9–10 weeks of age (Tanimura et al., 2008; Menalled et al., 2014). T-maze test was conducted in a room at approximately 15 lux. The black Plexiglas T-maze with arms 33 cm high, 10 cm wide, and 49 cm long was filled with 25 ± 1°C water colored opaque with non-toxic white tempera paint. A platform was submerged approximately 0.5 cm below the water surface at one end of the left or right arm. In the acquisition phase, mice were placed in the stem of the water-filled T-maze and were allowed to swim to find the hidden escape platform in either the right or left arm. The location of the platform was fixed for each mouse. Once a mouse reached the hidden platform, the mouse was allowed to stay there for 10 s. The mice underwent 8 trials per day with an approximately 15 min of inter-trial interval. If a mouse reached the platform in 6 or more out of 8 trials per day for 2 consecutive days, the mouse met the criteria and the number of days required to meet the criteria was counted. Up to 7 days were provided to achieve the criteria in the acquisition phase and mice that did not reach the criteria within 7 days were assigned a value of 7 (cut-off value). Once the criteria were achieved within 7 days, each

mouse was advanced to the reversal phase. In the reversal phase, the platform was located in the opposite arm for each mouse. The performance in this phase was assessed for 6 consecutive days (8 trials per day).

Seizure Susceptibility. Seizures were observed in R6/2 mice during the first 3 days of the acquisition phase when we tried to conduct water T-maze test. These seizures were probably caused by water-immersion stress because R6/2 mice are known to have increased susceptibility to seizures triggered by stress (Mangiarini et al., 1996). The number of observed seizures during those days was counted.

Contextual Fear Conditioning (CFC) Test. To evaluate contextual memory, we conducted a contextual fear conditioning task in mice at 11 weeks of age. Training was performed using an automated software package (Coulbourn, Whitehall, PA). On the training day, mice were acclimated to the testing chamber for 20 s before receiving the first of 5 presentations of 2-s footshock (0.6 mA). The baseline data were recorded during the first shock. The second shock was presented 80 s later; the third and fourth shocks were presented 120 s after the second and third shock, respectively. The final shock was presented 140 s after the fourth shock. Mice were then left in the chambers for 40 s and subsequently returned to their home cages. On the test day, mice were placed back in the original training context for a 3-min period 24 h later

from the training. Contextual memory was assessed by measuring a freezing behavior, defined as cessation of all movement with the exception of respiration. Freezing behavior was quantified using software, FreezeFrame (Actimetrics, Wilmette, IL).

Statistical Analysis. The statistical significance of differences between two groups was analyzed using Aspin–Welch test with an alpha level of 0.05. For comparing dose-dependent effects of multiple doses of TAK-063 with the control group, the homogeneity of variances was assessed by Bartlett's test, and then the statistical significance was analyzed using two-tailed Williams' test (Williams, 1971) (for parametric data, $P > 0.05$ by Bartlett's test) or two-tailed Shirley-Williams test (Shirley, 1977) (for non-parametric data, $P \leq 0.05$ by Bartlett's test). Differences yielding $P \leq 0.05$ were considered significant. In the clasping test, we scored "1" or "0" when each mouse exhibited full clasping behavior or not, respectively, and the statistical significance was analyzed using two-tailed Shirley-Williams test. In the rotarod test, differences between vehicle-treated WT mice and vehicle-treated R6/2 mice at each week of age were analyzed using a repeated measures analysis of variance (RM-ANOVA) with test day as the repeated factor.

Results

TAK-063 Suppressed BDNF Reduction in the Striatum of R6/2 Mice. TAK-063

dose-dependently increased cAMP and cGMP levels, and upregulated phosphorylation of CREB in the mouse striatum (Suzuki et al., 2015). TAK-063 at 0.5 mg/kg (51% striatal PDE10A occupancy) significantly increased cAMP and cGMP levels in the mouse striatum after both single and repeated administration (Suzuki et al., 2015; Suzuki et al., 2016). Thus, 0.5 mg/kg and a higher dose (5 mg/kg, 91% PDE10A occupancy in mice) of TAK-063 were used in this study. Daily oral administration of vehicle or TAK-063 at 0.5 mg/kg or 5 mg/kg was started from 4.5–5 to 12 weeks of age. Activation of cAMP signaling cascades is known to upregulate BDNF expression via phosphorylation of CREB (Tardito et al., 2006). We evaluated BDNF protein levels in the striatum and the cortex of mice at 12 weeks of age. BDNF levels in the striatum of vehicle-treated R6/2 mice were significantly lower than that of vehicle-treated WT mice ($P \leq 0.01$; Fig. 1A), and 8 weeks of daily treatment with TAK-063 significantly and dose-dependently suppressed the reduction of BDNF levels in R6/2 mice ($P \leq 0.05$; Fig. 1A). BDNF levels in the cortex of vehicle-treated R6/2 mice were not statistically different from those of vehicle-treated WT mice ($P = 0.15$). Repeated treatment with TAK-063 did not statistically change the BDNF levels in the cortex of R6/2 mice ($P = 0.06$, Fig. 1B).

TAK-063 Prevented Striatal Atrophy in R6/2 Mice. Significant upregulation of BDNF levels in the striatum by TAK-063 was expected to produce a neuroprotective effect against

mutant huntingtin-induced neurodegeneration in R6/2 mice. Striatal atrophy in R6/2 mice was assessed by measuring striatal areas in the Nissl-stained brain sections of mice at 12 weeks of age (Fig. 2A). The area of the striatum was significantly reduced in brain sections from vehicle-treated R6/2 mice compared with those from vehicle-treated WT mice ($P \leq 0.01$; Fig. 2B). Repeated treatment with TAK-063 at 5 mg/kg/day significantly inhibited the decline of striatal area in R6/2 mice ($P \leq 0.05$ at 5 mg/kg/day; Fig. 2B). This result suggests that TAK-063 prevents striatal atrophy in R6/2 mice.

TAK-063 Reduced Seizure Frequency but Did Not Prevent the Suppression of Body Weight Gain in R6/2 Mice. We assessed effects of repeated treatment with TAK-063 on general symptoms seen in R6/2 mice, including the suppression of body weight gain and increased susceptibility to seizures. The body weight of vehicle-treated WT mice increased gradually up to 11 weeks of age, whereas that of vehicle-treated R6/2 mice reached a plateau at 7 weeks of age (Fig. 3A). At 12 weeks of age, the body weight of vehicle-treated R6/2 mice was significantly lower than that of vehicle-treated WT mice ($P \leq 0.01$). Repeated treatment with TAK-063 did not significantly prevent the suppression of body weight gain in R6/2 mice. Seizures were observed in R6/2 mice during the first 3 days of the acquisition phase when we tried to conduct water T-maze test at 9 weeks of age. These seizures were probably caused by water-immersion stress because R6/2 mice are known to have increased susceptibility to

seizures triggered by stress (Mangiarini et al., 1996). Repeated treatment of TAK-063 dose-dependently and significantly suppressed seizure frequency in R6/2 mice ($P \leq 0.05$ at 5 mg/kg/day; Fig. 3B).

TAK-063 Prevented Motor Deficits in R6/2 Mice. To evaluate the effects of TAK-063 on motor functions in R6/2 mice, we assessed the development of a clasping behavior and performed open field test and rotarod test. The foot clasping, an abnormal posturing of the hind limb during the tail suspension (Nguyen et al., 2005), is a cardinal phenotype in R6/2 mice (Mangiarini et al., 1996). We assessed foot clasping behavior weekly from 5 to 12 weeks of age. Vehicle-treated R6/2 mice, but not WT mice, exhibited clasping behavior after 8 weeks of age (Fig. 4A). TAK-063 at 5 mg/kg/day tended to decrease the percentage of mice exhibiting clasping behavior at 10 and 11 weeks of age ($P = 0.07$ and 0.10, respectively), although the difference did not reach statistical significance (Fig. 4A). In open field test, vehicle-treated R6/2 mice showed significant decreases of total distance traveled and rearing frequency compared with vehicle-treated WT mice at 12 weeks of age (Fig. 4B and 4C). Repeated treatment with TAK-063 dose-dependently inhibited the decrease of total distance traveled and rearing frequency ($P \leq 0.05$ at 5 mg/kg/day; Fig. 4B and 4C). In rotarod test, R6/2 mice exhibited decrease of latency to fall off from the rotarod at 6 and 12 weeks of age, indicating the deficit in motor coordination (Fig. 4D). RM-ANOVA between WT and

vehicle-treated R6/2 mice at each week of age showed significant effects of genotype at 6 and 12 weeks of age ($P \leq 0.01$). Repeated treatment with TAK-063 did not prevent this deficit under these experimental conditions (Fig. 4D). These results suggest that in R6/2 mice, TAK-063 prevents the deficits in motor functions, including the development of clasping behavior and the decreased activities in open field, but not the deficits in motor coordination on rotarod.

TAK-063 Prevented Procedural Learning Deficits in Procedural Water T-Maze Test in R6/2 Mice. To assess the efficacy of TAK-063 for cognitive impairments in R6/2 mice, we conducted procedural water T-maze test at 9 to 10 weeks of age. In this test, procedural learning and cognitive flexibility can be evaluated in the acquisition and reversal phase, respectively (Tanimura et al., 2008). This task is especially useful in assessing cognitive function in animals with motor impairments since the accuracy of their “choices” can be measured independently of their latency of escape, which may be perturbed by poor swimming performance (Melief et al., 2015). Vehicle-treated R6/2 mice needed more days to reach the criteria than vehicle-treated WT mice in the acquisition phase, indicating impaired procedural learning in R6/2 mice ($P \leq 0.01$; Fig. 5A). Repeated treatment with TAK-063 dose-dependently and significantly reduced the numbers of days required to meet the criteria in R6/2 mice, suggesting the partial improvement in procedural learning by a high dose of

TAK-063 ($P \leq 0.05$ at 5 mg/kg/day; Fig. 5A).

Once the criteria were achieved within 7 days, the animals progressed to the reversal phase on an individual basis to characterize their cognitive flexibility. Eleven mice in each R6/2 mice group did not reach the criteria even after 7 days of acquisition phase and therefore were not evaluated in the reversal phase. On day 1 in the reversal phase, starting performance was different between groups. To assess the improvement in performance during the reversal phase, correct choice percentages on the latter half of this phase (days 4 to 6) were averaged and normalized by those on day 1. These values were represented as normalized correct choice percentages. The normalized correct choice percentages were significantly lower in R6/2 mice than WT mice in the reversal phase, suggesting impaired cognitive flexibility in R6/2 mice ($P \leq 0.05$; Fig. 5B). Repeated administration of TAK-063 tended to increase the normalized correct choice percentages, although the effect did not reach statistical significance ($P = 0.09$ at 5 mg/kg/day; Fig. 5B). These results suggest that the high dose of TAK-063 (5 mg/kg/day) partially prevents procedural learning deficits, whereas it does not have significant effects on the impairments of cognitive flexibility in R6/2 mice.

TAK-063 Did Not Prevent Contextual Memory Deficits in CFC Test in R6/2 Mice. To evaluate effects of TAK-063 on contextual memory deficits in R6/2 mice, we conducted CFC test at 11 weeks of age. At the contextual phase 24 h after conditioning session, freezing

behavior was significantly decreased in vehicle-treated R6/2 mice compared with vehicle-treated WT mice, indicating severe impairment of associative learning in R6/2 mice ($P \leq 0.01$; Fig. 6). Repeated administration of TAK-063 did not increase the freezing time in R6/2 mice at the contextual phase. This result suggests that TAK-063 does not prevent contextual memory deficits in R6/2 mice at 11 weeks of age.

Discussion

Indirect pathway MSNs appear to be more vulnerable than direct pathway MSNs in patients with HD (Galvan et al., 2012). These differences in MSN vulnerability may provide unique opportunities in the future treatment of HD. Compared with other PDE10A inhibitors such as MP-10 and compound 1, TAK-063 with a faster off-rate property activates the indirect pathway MSNs to a similar extent, whereas it partially activates the direct pathway MSNs (Suzuki et al., 2016). This activation pattern of MSNs by TAK-063 may protect MSNs in both pathways from neurotoxic effects of mutant huntingtin without inducing unbalanced activation of these neural pathways. We evaluated the effects of TAK-063 on striatal neurodegeneration and behavioral deficits in the R6/2 mouse model of HD. The results were summarized and compared with the reported effects of TP-10 (Table 1).

BDNF plays a critical role in activity and survival of MSNs (Choi et al., 2009). Striatal BDNF levels were decreased in R6/2 mice, and repeated treatment with TAK-063 at 5

mg/kg/day almost completely prevented this reduction of BDNF levels at 12 weeks of age. Moreover, TAK-063 at 5 mg/kg/day significantly prevented striatal atrophy in R6/2 mice at this age. These results suggest that the indirect pathway MSN-biased activation pattern by TAK-063 is neuroprotective in the striatum of R6/2 mice. In addition, administration of TAK-063 prevented the development of clasping behavior and deficits in motor functions in the open field, suggesting the prevention of disease progression in R6/2 mice. TAK-063 did not prevent the progressive deficit in motor coordination in rotarod test under these experimental conditions. Further studies would be needed but the impairment of motor coordination may be due to some functional deficits of the surviving MSNs, other brain regions, or peripheral regions.

The striatum and cortex are highly connected via neural circuitry (Haber, 2003; Simpson et al., 2010), and this connectivity of the corticostriatal circuit enables sensory inputs to be associated with the output functions such as motor and cognitive responses, including procedural learning and cognitive flexibility (Tanimura et al., 2008). Pharmacological magnetic resonance imaging and electroencephalography studies suggest that TAK-063 likely modulates cortical activity through cortical-striatal-thalamic circuits (Y. Tomimatsu, D. Cash, M. Suzuki, K. Suzuki, M. Bernanos, C. Simmons, S. Williams, and H. Kimura, manuscript in preparation). TAK-063 at 0.3 mg/kg improved cognitive functions in several rodent models (Shiraishi et al., 2016). Therefore, in addition to neuroprotective effects of TAK-063,

modulation of cortical functions through the corticostriatal circuit may also contribute to the improvement of cognitive function of R6/2 mice in the procedural water T-maze test. TAK-063 did not prevent the deficit in contextual memory in R6/2 mice in CFC test at 11 weeks of age. The hippocampus plays an important role in the formation of contextual memory (Ramirez et al., 2013). Autoradiography study using rat brain sections suggests that the PDE10A expression level in the hippocampus is quite low: 40-fold lower levels than that in the striatum (Harada et al., 2015). In addition, acute treatment with TAK-063 did not increase cAMP and pCREB levels in the mouse hippocampus (Suzuki et al., 2015). Thus, TAK-063 does not show significant improvement in contextual memory deficits in CFC test in R6/2 mice.

R6/2 mice are known to develop a tremor that worsens under stress and increases susceptibility to seizures (Mangiarini et al., 1996; Cepeda-Prado et al., 2012). The seizures observed in R6/2 mice during the procedural water T-maze test were probably triggered by the stress of water immersion. Intriguingly, TAK-063 dose-dependently decreased seizure frequency. HD patients with more than 60 CAG repeats are afflicted by early and more aggressive pathologies, including myoclonic seizures, which are refractory to standard antiepileptic medications (Naydenov et al., 2014). TAK-063 could also have a potential therapeutic effect on myoclonic seizures in severe HD patients.

TAK-063 did not prevent the suppression of body weight gain in R6/2 mice. TP-10 also

showed no effects on it in R6/2 mice (Giampà et al., 2010). Although the underlying mechanism of the suppression of body weight gain in mouse models of HD and in patients with HD remains unclear, peripheral effects of mutant huntingtin including wasting of skeletal muscle and adipose tissue are hypothesized (van der Burg et al., 2009). PDE10A is selectively expressed in MSNs of the striatum; thus, if the suppression of body weight gain were due to peripheral effects of mutant huntingtin it would be reasonable that selective inhibition of PDE10A would have low impact on the suppression of body weight gain by mutant huntingtin in R6/2 mice.

TAK-063 did not prevent the progressive deficit in motor coordination in a rotarod test under the present experimental conditions, whereas TP-10 was reported to significantly prevent the decline in rotarod performance in R6/2 mice (Giampà et al., 2010). Although the precise reasons for this discrepancy remain unclear, differences in experimental conditions could possibly influence the pharmacological effects of the two compounds: animal husbandry and the acceleration and the maximum speed of rotarod are not consistent with those in TP-10 study. In line with this speculation, coenzyme Q10 and minocycline, potential drug candidates for the treatment of HD, produced conflicting results regarding their efficacy in rotarod test in R6/2 mice at least partially due to animal husbandry and testing protocols (Menalled et al., 2010). To further investigate the differences of effects on impairment in motor coordination between TAK-063 and TP-10, a direct comparison study under same

experimental conditions is needed.

Some current antipsychotics with dopamine D_2 receptor antagonistic activity such as haloperidol and fluphenazine are commonly used to suppress chorea in HD by reducing involuntary movements through the activation of the indirect pathway (Giménez-Roldán and Mateo, 1989; Bonelli and Wenning, 2006). PDE10A inhibitors would also be expected to suppress chorea via PDE10A inhibition in the indirect pathway. However, PDE10A inhibitors activate both direct and indirect MSN pathways, and these pathways are considered to have competing effects on motor functions. In fact, a cataleptic response induced by activation of the indirect pathway by haloperidol was canceled by excessive activation of the direct pathway by a D_1 receptor agonist SKF82958 in rats (Suzuki et al., 2015). Moreover, several reports have suggested that excessive activation of the direct pathway MSNs is involved in the production of dystonia, one of the major clinical features of HD (Janavs and Aminoff, 1998; Louis et al., 1999; Burbaud, 2012). It is not known whether the indirect pathway MSN-biased activation pattern by TAK-063 would translate to therapeutic benefit in humans. Further preclinical and clinical studies are worth conducting to investigate pharmacological and tolerability profiles of TAK-063.

In this study, we used R6/2 mouse, a fragment Tg model, to evaluate the potential of TAK-063 on HD. The R6/2 mouse is a widely used mouse model of HD for a preclinical study, because this fragment Tg model has a robust phenotype with an early onset, rapidly

progressive neurodegeneration, weight loss, and motor and cognitive deficits (Pouladi et al., 2013). However, there are also some caveats to the use of fragment Tg models to determine the preclinical efficacy of potential therapeutic candidates: widespread and relatively nonselective neuropathology, and/or a too rapid disease progression which may reduce the ability to detect the efficacy of a test compound (William Yang and Gray, 2011). Knock-in mouse models, such as CAG140, are thought to possess better face and construct validity compared with fragment Tg models because knock-in mouse models have a slow progression of phenotype, have a similar neuropathology to that of HD, and are genetically more representative of the human disease under the endogenous huntingtin promoter (Menalled et al., 2003; Ferrante, 2009). Thus, knock-in mouse models are considered to be a more faithful genetic model of the human condition. Although a pharmacological evaluation using knock-in mouse models with a slower phenotype progression will require longer study periods than fragment Tg models, further study using knock-in mouse models may provide additional information about the therapeutic potential of TAK-063 in HD.

In summary, these results suggest that TAK-063 with the indirect pathway MSN-biased activation pattern protects striatal neurons from degeneration and ameliorates behavioral deficits in the R6/2 mouse model of HD. TAK-063 is currently in clinical development for the treatment of schizophrenia (ClinicalTrials.gov Identifier: NCT02477020).

Acknowledgments

We thank PsychoGenics Inc. for conducting behavioral experiments, Drug Metabolism and Pharmacokinetics Research Laboratories (Takeda Pharmaceutical Company Limited) for analysis of TAK-063 exposure and PDE10A occupancy, and Motohisa Suzuki (Takeda Pharmaceutical Company Limited) for the blind evaluation of histological data.

Authorship Contributions

Participated in research design: Suzuki, Kimura.

Conducted experiments: Harada, Suzuki.

Performed data analysis: Harada, Suzuki, Kimura.

Wrote or contributed to the writing of the manuscript: Harada, Suzuki, Kimura.

References

Bonelli RM and Wenning GK (2006) Pharmacological management of Huntington's disease: an evidence-based review. *Curr Pharm Des* **12**:2701-2720.

Burbaud P (2012) Dystonia Pathophysiology: A Critical Review.199-220.

Cepeda-Prado E, Popp S, Khan U, Stefanov D, Rodríguez J, Menalled LB, Dow-Edwards D, Small SA and Moreno H (2012) R6/2 Huntington's disease mice develop early and progressive abnormal brain metabolism and seizures. *J Neurosci* **32**:6456-6467.

Choi YS, Lee B, Cho HY, Reyes IB, Pu XA, Saido TC, Hoyt KR and Obrietan K (2009) CREB is a key regulator of striatal vulnerability in chemical and genetic models of Huntington's disease. *Neurobiol Dis* **36**:259-268.

Coskran TM, Morton D, Menniti FS, Adamowicz WO, Kleiman RJ, Ryan AM, Strick CA, Schmidt CJ and Stephenson DT (2006) Immunohistochemical localization of phosphodiesterase 10A in multiple mammalian species. *J Histochem Cytochem* **54**:1205-1213.

Crook ZR and Housman DE (2012) Dysregulation of dopamine receptor D2 as a sensitive measure for Huntington disease pathology in model mice. *Proc Natl Acad Sci U S A* **109**:7487-7492.

Ferrante RJ (2009) Mouse models of Huntington's disease and methodological considerations for therapeutic trials. *Biochim Biophys Acta* **1792**:506-520.

Frank S (2014) Treatment of Huntington's disease. *Neurotherapeutics* **11**:153-160.

Fujishige K, Kotera J, Michibata H, Yuasa K, Takebayashi S, Okumura K and Omori K (1999) Cloning and characterization of a novel human phosphodiesterase that hydrolyzes both cAMP and cGMP (PDE10A). *J Biol Chem* **274**:18438-18445.

Galvan L, André VM, Wang EA, Cepeda C and Levine MS (2012) Functional Differences Between Direct and Indirect Striatal Output Pathways in Huntington's Disease. *J Huntingtons Dis* **1**:17-25.

Giampà C, Laurenti D, Anzilotti S, Bernardi G, Menniti FS and Fusco FR (2010) Inhibition of the striatal specific phosphodiesterase PDE10A ameliorates striatal and cortical pathology in R6/2 mouse model of Huntington's disease. *PLoS One* **5**:e13417.

Giampà C, Patassini S, Borreca A, Laurenti D, Marullo F, Bernardi G, Menniti FS and Fusco FR (2009) Phosphodiesterase 10 inhibition reduces striatal excitotoxicity in the quinolinic acid model of Huntington's disease. *Neurobiol Dis* **34**:450-456.

Giménez-Roldán S and Mateo D (1989) [Huntington disease: tetrabenazine compared to haloperidol in the reduction of involuntary movements]. *Neurologia* **4**:282-287.

Gines S, Seong IS, Fossale E, Ivanova E, Trettel F, Gusella JF, Wheeler VC, Persichetti F and MacDonald ME (2003) Specific progressive cAMP reduction implicates energy deficit in presymptomatic Huntington's disease knock-in mice. *Hum Mol Genet* **12**:497-508.

Glass M, Dragunow M and Faull RL (2000) The pattern of neurodegeneration in Huntington's

disease: a comparative study of cannabinoid, dopamine, adenosine and GABA(A) receptor alterations in the human basal ganglia in Huntington's disease. *Neuroscience* **97**:505-519.

Graybiel AM (1990) Neurotransmitters and neuromodulators in the basal ganglia. *Trends Neurosci* **13**:244-254.

Graybiel AM (2000) The basal ganglia. *Curr Biol* **10**:R509-511.

Haber SN (2003) The primate basal ganglia: parallel and integrative networks. *J Chem Neuroanat* **26**:317-330.

Harada A, Suzuki K, Kamiguchi N, Miyamoto M, Tohyama K, Nakashima K, Taniguchi T and Kimura H (2015) Characterization of Binding and Inhibitory Properties of TAK-063, a Novel Phosphodiesterase 10A Inhibitor. *PLoS One* **10**:e0122197.

Janavs JL and Aminoff MJ (1998) Dystonia and chorea in acquired systemic disorders. *J Neurol Neurosurg Psychiatry* **65**:436-445.

Kunitomo J, Yoshikawa M, Fushimi M, Kawada A, Quinn JF, Oki H, Kokubo H, Kondo M, Nakashima K, Kamiguchi N, Suzuki K, Kimura H and Taniguchi T (2014) Discovery of

1-[2-fluoro-4-(1H-pyrazol-1-yl)phenyl]-5-methoxy-3-(1-phenyl-1H-pyrazol-5-yl)pyri dazin-4(1H)-one (TAK-063), a highly potent, selective, and orally active phosphodiesterase 10A (PDE10A) inhibitor. *J Med Chem* **57**:9627-9643.

Louis ED, Lee P, Quinn L and Marder K (1999) Dystonia in Huntington's disease: prevalence and clinical characteristics. *Mov Disord* **14**:95-101.

Lüesse HG, Schiefer J, Spruenken A, Puls C, Block F and Kosinski CM (2001) Evaluation of R6/2 HD transgenic mice for therapeutic studies in Huntington's disease: behavioral testing and impact of diabetes mellitus. *Behav Brain Res* **126**:185-195.

Mangiarini L, Sathasivam K, Seller M, Cozens B, Harper A, Hetherington C, Lawton M, Trottier Y, Lehrach H, Davies SW and Bates GP (1996) Exon 1 of the HD gene with an expanded CAG repeat is sufficient to cause a progressive neurological phenotype in transgenic mice. *Cell* **87**:493-506.

Mantamadiotis T, Lemberger T, Bleckmann SC, Kern H, Kretz O, Martin Villalba A, Tronche F, Kellendonk C, Gau D, Kapfhammer J, Otto C, Schmid W and Schutz G (2002) Disruption of CREB function in brain leads to neurodegeneration. *Nat Genet* **31**:47-54.

Melief EJ, Cudaback E, Jorstad NL, Sherfield E, Postupna N, Wilson A, Darvas M, Montine KS, Keene CD and Montine TJ (2015) Partial depletion of striatal dopamine enhances penetrance of cognitive deficits in a transgenic mouse model of Alzheimer's disease. *J Neurosci Res* **93**:1413-1422.

Menalled LB, Kudwa AE, Oakeshott S, Farrar A, Paterson N, Filippov I, Miller S, Kwan M, Olsen M, Beltran J, Torello J, Fitzpatrick J, Mushlin R, Cox K, McConnell K,

Mazzella M, He D, Osborne GF, Al-Nackkash R, Bates GP, Tuunanen P, Lehtimaki K, Brunner D, Ghavami A, Ramboz S, Park L, Macdonald D, Munoz-Sanjuan I and Howland D (2014) Genetic deletion of transglutaminase 2 does not rescue the phenotypic deficits observed in R6/2 and zQ175 mouse models of Huntington's disease. *PLoS One* **9**:e99520.

Menalled LB, Patry M, Ragland N, Lowden PA, Goodman J, Minnich J, Zahasky B, Park L, Leeds J, Howland D, Signer E, Tobin AJ and Brunner D (2010) Comprehensive behavioral testing in the R6/2 mouse model of Huntington's disease shows no benefit from CoQ10 or minocycline. *PLoS One* **5**:e9793.

Menalled LB, Sison JD, Dragatsis I, Zeitlin S and Chesselet MF (2003) Time course of early motor and neuropathological anomalies in a knock-in mouse model of Huntington's disease with 140 CAG repeats. *J Comp Neurol* **465**:11-26.

Naydenov AV, Horne EA, Cheah CS, Swinney K, Hsu KL, Cao JK, Marrs WR, Blankman JL, Tu S, Cherry AE, Fung S, Wen A, Li W, Saporito MS, Selley DE, Cravatt BF, Oakley JC and Stella N (2014) ABHD6 blockade exerts antiepileptic activity in PTZ-induced seizures and in spontaneous seizures in R6/2 mice. *Neuron* **83**:361-371.

Nguyen T, Hamby A and Massa SM (2005) Clioquinol down-regulates mutant huntingtin expression in vitro and mitigates pathology in a Huntington's disease mouse model. *Proc Natl Acad Sci U S A* **102**:11840-11845.

Nishi A, Kuroiwa M, Miller DB, O'Callaghan JP, Bateup HS, Shuto T, Sotogaku N, Fukuda T, Heintz N, Greengard P and Snyder GL (2008) Distinct roles of PDE4 and PDE10A in the regulation of cAMP/PKA signaling in the striatum. *J Neurosci* **28**:10460-10471.

Norris PJ, Waldvogel HJ, Faull RL, Love DR and Emson PC (1996) Decreased neuronal nitric oxide synthase messenger RNA and somatostatin messenger RNA in the striatum of Huntington's disease. *Neuroscience* **72**:1037-1047.

Nucifora FC, Jr., Sasaki M, Peters MF, Huang H, Cooper JK, Yamada M, Takahashi H, Tsuji S, Troncoso J, Dawson VL, Dawson TM and Ross CA (2001) Interference by huntingtin and atrophin-1 with cbp-mediated transcription leading to cellular toxicity. *Science* **291**:2423-2428.

Padovan-Neto FE, Sammut S, Chakroborty S, Dec AM, Threlfell S, Campbell PW, Mudrakola V, Harms JF, Schmidt CJ and West AR (2015) Facilitation of corticostriatal transmission following pharmacological inhibition of striatal phosphodiesterase 10A: role of nitric oxide-soluble guanylyl cyclase-cGMP signaling pathways. *J Neurosci* **35**:5781-5791.

Paxinos G and Franklin KBJ (2001) *The mouse brain in stereotaxic coordinates*, 2nd ed. Academic Press, San Diego.

Pouladi MA, Morton AJ and Hayden MR (2013) Choosing an animal model for the study of Huntington’s disease. *Nat Rev Neurosci* **14**:708-721.

Ramirez S, Tonegawa S and Liu X (2013) Identification and optogenetic manipulation of memory engrams in the hippocampus. *Front Behav Neurosci* **7**:226.

Reiner A, Albin RL, Anderson KD, D'Amato CJ, Penney JB and Young AB (1988) Differential loss of striatal projection neurons in Huntington disease. *Proc Natl Acad Sci U S A* **85**:5733-5737.

Ross CA, Aylward EH, Wild EJ, Langbehn DR, Long JD, Warner JH, Scahill RI, Leavitt BR, Stout JC, Paulsen JS, Reilmann R, Unschuld PG, Wexler A, Margolis RL and Tabrizi SJ (2014) Huntington disease: natural history, biomarkers and prospects for therapeutics. *Nat Rev Neurol* **10**:204-216.

Ross CA and Tabrizi SJ (2011) Huntington's disease: from molecular pathogenesis to clinical treatment. *Lancet Neurol* **10**:83-98.

Sapp E, Ge P, Aizawa H, Bird E, Penney J, Young AB, Vonsattel JP and DiFiglia M (1995) Evidence for a preferential loss of enkephalin immunoreactivity in the external globus pallidus in low grade Huntington's disease using high resolution image analysis. *Neuroscience* **64**:397-404.

Seeger TF, Bartlett B, Coskran TM, Culp JS, James LC, Krull DL, Lanfear J, Ryan AM, Schmidt CJ, Strick CA, Varghese AH, Williams RD, Wylie PG and Menniti FS (2003) Immunohistochemical localization of PDE10A in the rat brain. *Brain Res* **985**:113-126.

Shiraishi E, Suzuki K, Harada A, Suzuki N and Kimura H (2016) The Phosphodiesterase 10A Selective Inhibitor TAK-063 Improves Cognitive Functions Associated with Schizophrenia in Rodent Models. *J Pharmacol Exp Ther* **356**:587-595.

Shirley E (1977) A non-parametric equivalent of Williams' test for contrasting increasing dose levels of a treatment. *Biometrics* **33**:386-389.

Simpson EH, Kellendonk C and Kandel E (2010) A possible role for the striatum in the pathogenesis of the cognitive symptoms of schizophrenia. *Neuron* **65**:585-596.

Slow EJ, van Raamsdonk J, Rogers D, Coleman SH, Graham RK, Deng Y, Oh R, Bissada N, Hossain SM, Yang YZ, Li XJ, Simpson EM, Gutekunst CA, Leavitt BR and Hayden MR (2003) Selective striatal neuronal loss in a YAC128 mouse model of Huntington disease. *Hum Mol Genet* **12**:1555-1567.

Sugars KL and Rubinsztein DC (2003) Transcriptional abnormalities in Huntington disease. *Trends Genet* **19**:233-238.

Suzuki K, Harada A, Shiraishi E and Kimura H (2015) In Vivo Pharmacological Characterization of TAK-063, a Potent and Selective Phosphodiesterase 10A Inhibitor with Antipsychotic-Like Activity in Rodents. *J Pharmacol Exp Ther* **352**:471-479.

Suzuki K, Harada A, Suzuki H, Miyamoto M and Kimura H (2016) TAK-063, a PDE10A Inhibitor with Balanced Activation of Direct and Indirect Pathways, Provides Potent Antipsychotic-Like Effects in Multiple Paradigms. *Neuropsychopharmacology*

41:2252-2262.

Tanimura Y, Yang MC and Lewis MH (2008) Procedural learning and cognitive flexibility in a mouse model of restricted, repetitive behaviour. *Behav Brain Res* **189**:250-256.

Tardito D, Perez J, Tiraboschi E, Musazzi L, Racagni G and Popoli M (2006) Signaling pathways regulating gene expression, neuroplasticity, and neurotrophic mechanisms in the action of antidepressants: a critical overview. *Pharmacol Rev* **58**:115-134.

Threlfell S, Sammut S, Menniti FS, Schmidt CJ and West AR (2009) Inhibition of Phosphodiesterase 10A Increases the Responsiveness of Striatal Projection Neurons to Cortical Stimulation. *J Pharmacol Exp Ther* **328**:785-795.

van der Burg JM, Björkqvist M and Brundin P (2009) Beyond the brain: widespread pathology in Huntington's disease. *Lancet Neurol* **8**:765-774.

Vonsattel JP and DiFiglia M (1998) Huntington disease. *J Neuropathol Exp Neurol* **57**:369-384.

Walker FO (2007) Huntington's disease. *The Lancet* **369**:218-228.

William Yang X and Gray M (2011) Mouse Models for Validating Preclinical Candidates for Huntington's Disease, in *Neurobiology of Huntington's Disease: Applications to Drug Discovery* (Lo DC and Hughes RE eds), CRC Press/Taylor & Francis Llc., Boca Raton (FL).

Williams DA (1971) A test for differences between treatment means when several dose levels

are compared with a zero dose control. *Biometrics* **27**:103-117.

Wilson JM, Ogden AM, Loomis S, Gilmour G, Baucum AJ, 2nd, Belecky-Adams TL and Merchant KM (2015) Phosphodiesterase 10A inhibitor, MP-10 (PF-2545920), produces greater induction of c-Fos in dopamine D2 neurons than in D1 neurons in the neostriatum. *Neuropharmacology* **99**:379-386.

Wyttenbach A, Swartz J, Kita H, Thykjaer T, Carmichael J, Bradley J, Brown R, Maxwell M, Schapira A, Orntoft TF, Kato K and Rubinsztein DC (2001) Polyglutamine expansions cause decreased CRE-mediated transcription and early gene expression changes prior to cell death in an inducible cell model of Huntington's disease. *Hum Mol Genet* **10**:1829-1845.

Footnotes

This work was funded by Takeda Pharmaceutical Company Limited.

All authors are employees of Takeda Pharmaceutical Company Limited.

Figure Legends

Fig. 1. Effects of TAK-063 on brain-derived neurotrophic factor (BDNF) levels in R6/2 mouse brain. BDNF protein levels in the striatum (A) and the cortex (B) of wild-type (WT) and R6/2 mice were measured by enzyme-linked immuno-sorbent assay at 12 weeks of age. Data are shown as mean + S.E.M. (n = 6 in each group). Statistical significance between WT and R6/2 mice was determined using Aspin–Welch test (**$P \leq 0.01$; versus vehicle-treated WT mice). Dose-dependent effects were statistically analyzed using two-tailed Williams' test (#$P \leq 0.05$; versus vehicle-treated R6/2 mice).

Fig. 2. Effects of TAK-063 on striatal atrophy in R6/2 mice. (A) Representative Nissl-stained coronal sections from mouse brains prepared at 12 weeks of age are shown. The dotted lines outline the striatum. (B) Striatal areas (mm^2) in the sections were measured to evaluate striatal atrophy. Data are represented as mean + S.E.M. (n = 4 in each group). Statistical significance between wild-type (WT) and R6/2 mice was determined using Aspin–Welch test (*$P \leq 0.05$; versus vehicle-treated WT mice). Dose-dependent effects were statistically analyzed using two-tailed Williams' test (#$P \leq 0.05$; versus vehicle-treated R6/2 mice).

Fig. 3. Effects of TAK-063 on body weight changes and seizure frequency in R6/2 mice. (A) Mice were weighed once per week throughout the study. Data are represented as mean ±

S.E.M. [n = 20 in vehicle-treated wild-type (WT) mice, n =19 vehicle-treated R6/2 mice, n = 22 in TAK-063-treated R6/2 mice]. At 12 weeks of age, the body weight of vehicle-treated R6/2 mice was significantly lower than that of vehicle-treated WT mice (**$P \leq 0.01$). Daily treatment with TAK-063 at 0.5 and 5 mg/kg/day for 8 weeks did not significantly prevent the suppression of body weight gain in R6/2 mice. Statistical significance between WT and R6/2 mice at 12 weeks of age was determined using Aspin–Welch test (**$P \leq 0.01$; versus vehicle-treated WT mice), and dose-dependent effects were statistically analyzed using two-tailed Williams' test (versus vehicle-treated R6/2 mice). (B) The number of seizures observed during the first 3 days of the acquisition phase in the procedural water T-maze test. All data are indicated as mean + S.E.M. (n = 20 in vehicle-treated WT mice, n =19 in vehicle-treated R6/2 mice, n = 22 in TAK-063-treated R6/2 mice). Dose-dependent effects were statistically analyzed using two-tailed Shirley–Williams test (#$P \leq 0.05$; versus vehicle-treated R6/2 mice).

Fig. 4. Effects of TAK-063 on motor deficits in R6/2 mice. (A) Clasping behavior was evaluated once per week at 5–12 weeks of age. Data are represented as the percentages of mice showing full clasping behavior within 30 s of tail suspension [n = 20 in vehicle-treated wild-type (WT) mice, n =19 in vehicle-treated R6/2 mice, n = 22 in TAK-063–treated R6/2 mice]. (B and C) An open field test was performed at 12 weeks of age. Locomotor activities

of mice were measured by two distinct indicators, total distance traveled (B) and rearing frequency (C). Data are represented as mean + S.E.M. (n = 20 in vehicle-treated WT mice, n =19 in vehicle-treated R6/2 mice, n = 22 in TAK-063-treated R6/2 mice). Statistical significance between WT and R6/2 mice was determined using Aspin–Welch test (**$P \leq 0.01$; versus vehicle-treated WT mice), and dose-dependent effects were statistically analyzed using two-tailed Shirley–Williams test (#$P \leq 0.05$; versus vehicle-treated R6/2 mice). (D) Motor coordination was assessed as the latency to fall off from a rotarod at 4, 6, and 12 weeks of age. Data are represented as mean ± S.E.M. (n = 20 in vehicle-treated WT mice, n =19 in vehicle-treated R6/2 mice, n = 22 in TAK-063–treated R6/2 mice). Differences between WT and vehicle-treated R6/2 mice at each week of age were analyzed using a repeated measures analysis of variance (RM-ANOVA). The RM-ANOVA showed a significant effect of test day at 4 weeks of age, significant effects of genotype and test day at 6 weeks of age, and significant effects of genotype and test day, and a significant genotype × test day interaction at 12 weeks of age. §§$P \leq 0.01$, a significant effect of genotype.

Fig. 5. Effects of TAK-063 on impairment of procedural learning and cognitive flexibility in a procedural water T-maze task in R6/2 mice at 9–10 weeks of age. (A) The number of days to reach criteria during the acquisition phase is shown. Repeated treatment with TAK-063 dose-dependently and significantly reduced the number of days required to meet the criteria in

R6/2 mice. Data are indicated as mean + S.E.M. [n = 20 in vehicle-treated wild-type (WT) mice, n =19 in vehicle-treated R6/2 mice, n = 22 in TAK-063-treated R6/2 mice]. Statistical significance between WT and R6/2 mice was determined using Aspin–Welch test (**$P \leq 0.01$; versus vehicle-treated WT mice). Dose-dependent effects were statistically analyzed using two-tailed Williams' test (#$P \leq 0.05$; versus vehicle-treated R6/2 mice). (B) Once the criteria were achieved within 7 days in the acquisition phase, the animals progressed to the reversal phase on an individual basis. Effects of repeated treatment with TAK-063 on reversal learning in R6/2 mice were evaluated. Data are expressed as the percentage of correct choices during days 4 to 6, normalized by the percent correct on Day 1, and are presented as mean + S.E.M. (n = 20 in vehicle-treated WT mice, n = 8 in vehicle-treated R6/2 mice, n = 11 in TAK-063–treated R6/2 mice). Statistical significance between WT and R6/2 mice was determined using Aspin–Welch (*$P \leq 0.05$; versus vehicle-treated WT mice).

Fig. 6. Effects of TAK-063 on memory deficits in a contextual fear conditioning (CFC) test in R6/2 mice at 11 weeks of age. Data are represented as percent freezing time relative to total measuring time (180 s), and indicated as mean + S.E.M. (n = 20 in vehicle-treated WT mice, n =19 in vehicle-treated R6/2 mice, n = 22 in TAK-063-treated R6/2 mice). Statistical significance between WT and R6/2 mice was determined using Aspin–Welch test (**$P \leq 0.01$; versus vehicle-treated WT mice).

JPET Fast Forward. Published on November 3, 2016 as DOI: 10.1124/jpet.116.237388
This article has not been copyedited and formatted. The final version may differ from this version.

TABLE 1

Comparison of the effects on the phenotypes of R6/2 mice between TAK-063 and TP-10.

		Effect of test compound	
		TAK-063	TP-10
Neural protection and brain pathology	Reduction of BDNF levels	Suppression (striatum)	Suppression (striatum and cortex)
	Striatal atrophy	Prevention	Prevention
	Formation of NIIs	NT	Reduction
	Microglial activation	NT	Inhibition
General behavior	Loss of righting reflex (survival)	NT	Inhibition
	Suppression of body weight gain	No effect	No effect
	Increase in seizure frequency	Suppression	NT
Motor function	Development of a clasping behavior	Prevention	Prevention
	Decrease in motor activity (open field test)	Inhibition	Inhibition
	Deficit in motor coordination	No effect	Improvement

	(rotarod test)		
Cognitive function	Deficits in procedural learning and cognitive flexibility (water T-maze test)	Improvement (procedural learning)	NT
	Deficit in contextual memory (contextual fear conditioning test)	No effect	NT

The results of TP-10 are reported by Giampà et al. (2010).

BDNF, brain-derived neurotrophic factor; NIIs, neuronal intranuclear inclusions; NT, not tested.

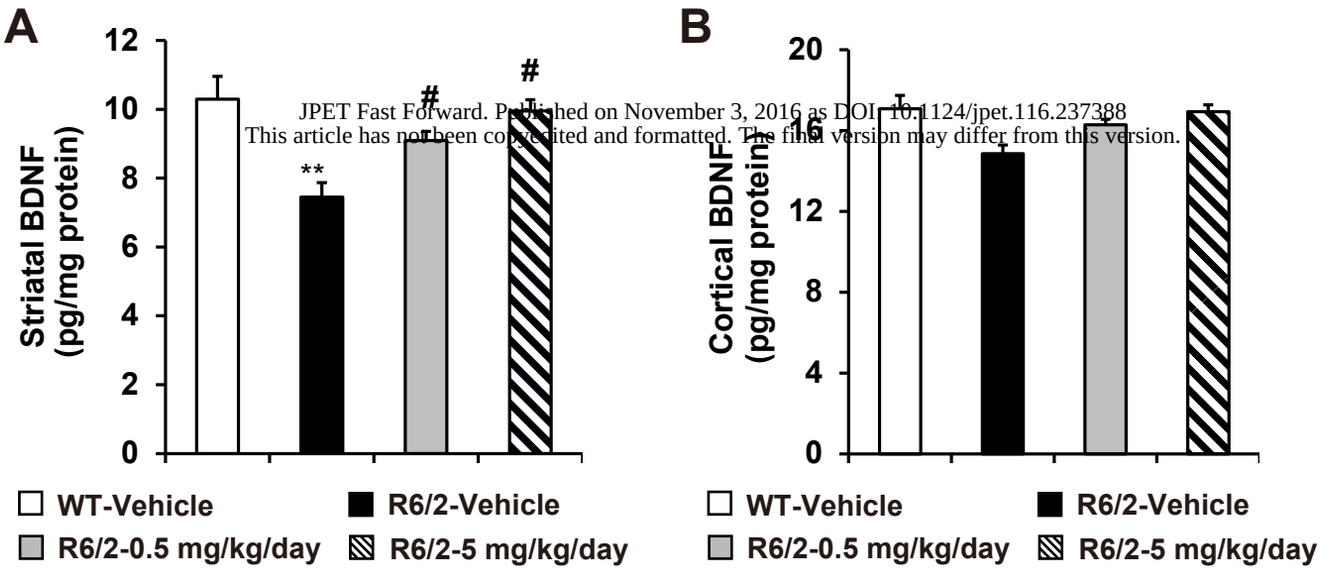

Figure 1

JPET Fast Forward. Published on November 3, 2016 as DOI: 10.1124/jpet.116.237388
This article has not been copyedited and formatted. The final version may differ from this version.

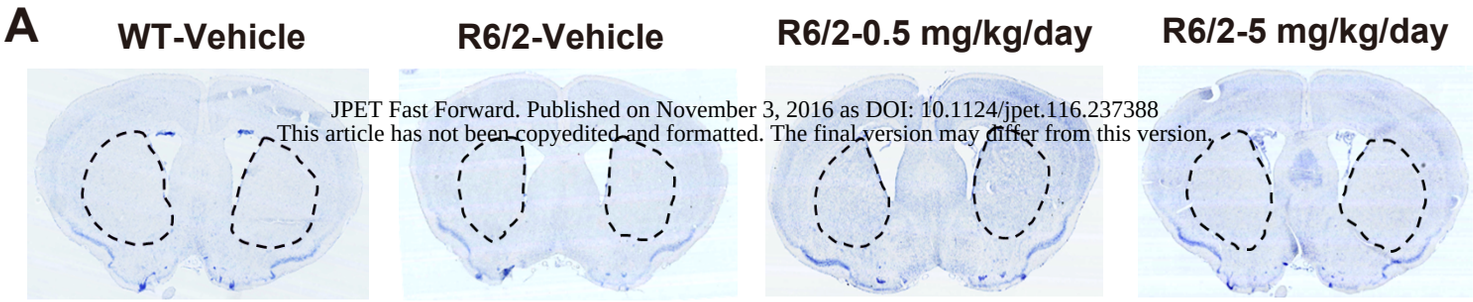

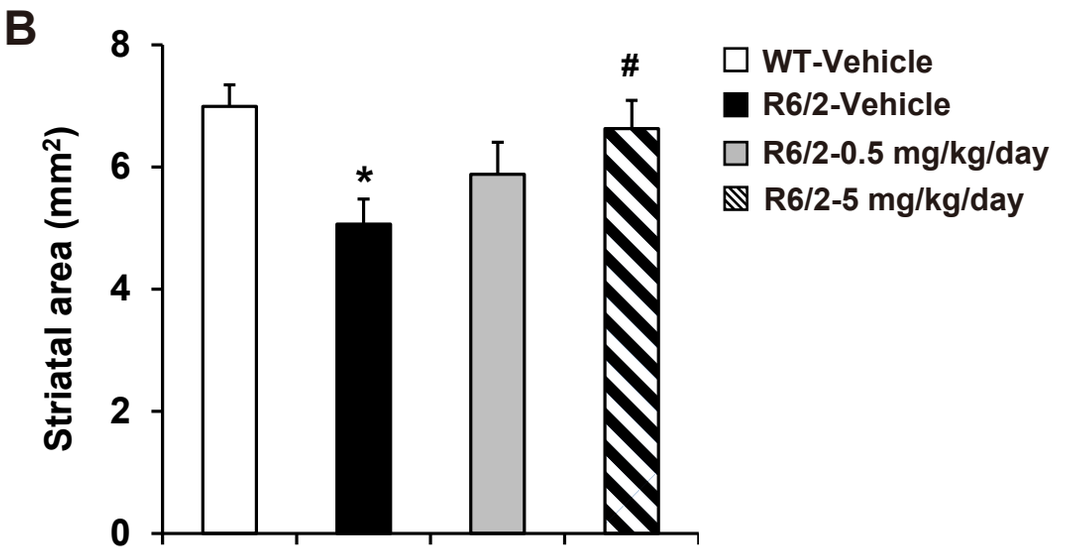

Figure 2

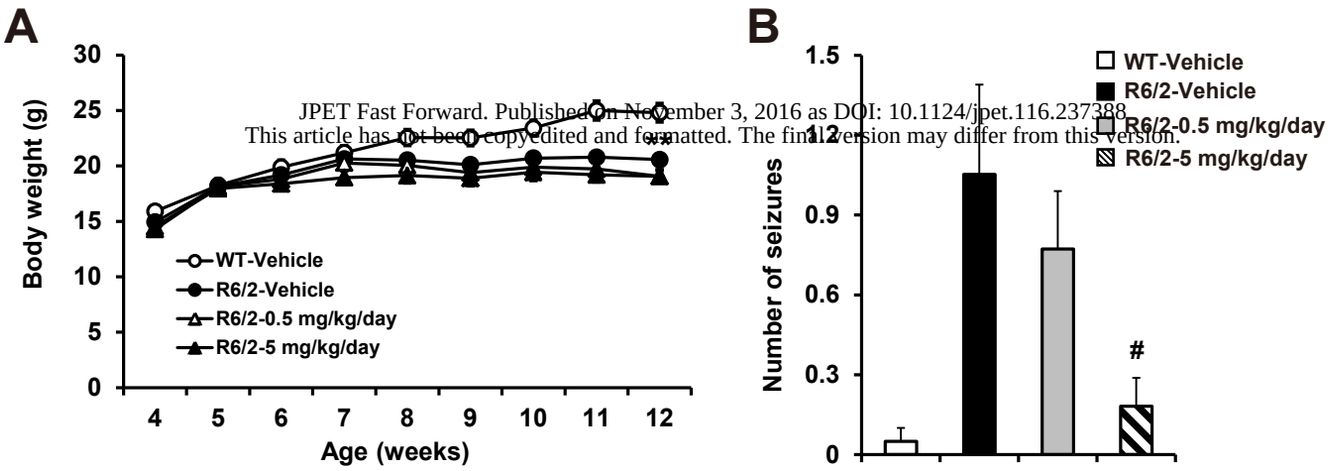

Figure 3

JPET Fast Forward. Published on November 3, 2016 as DOI: 10.1124/jpet.116.237388
This article has not been copyedited and formatted. The final version may differ from this version.

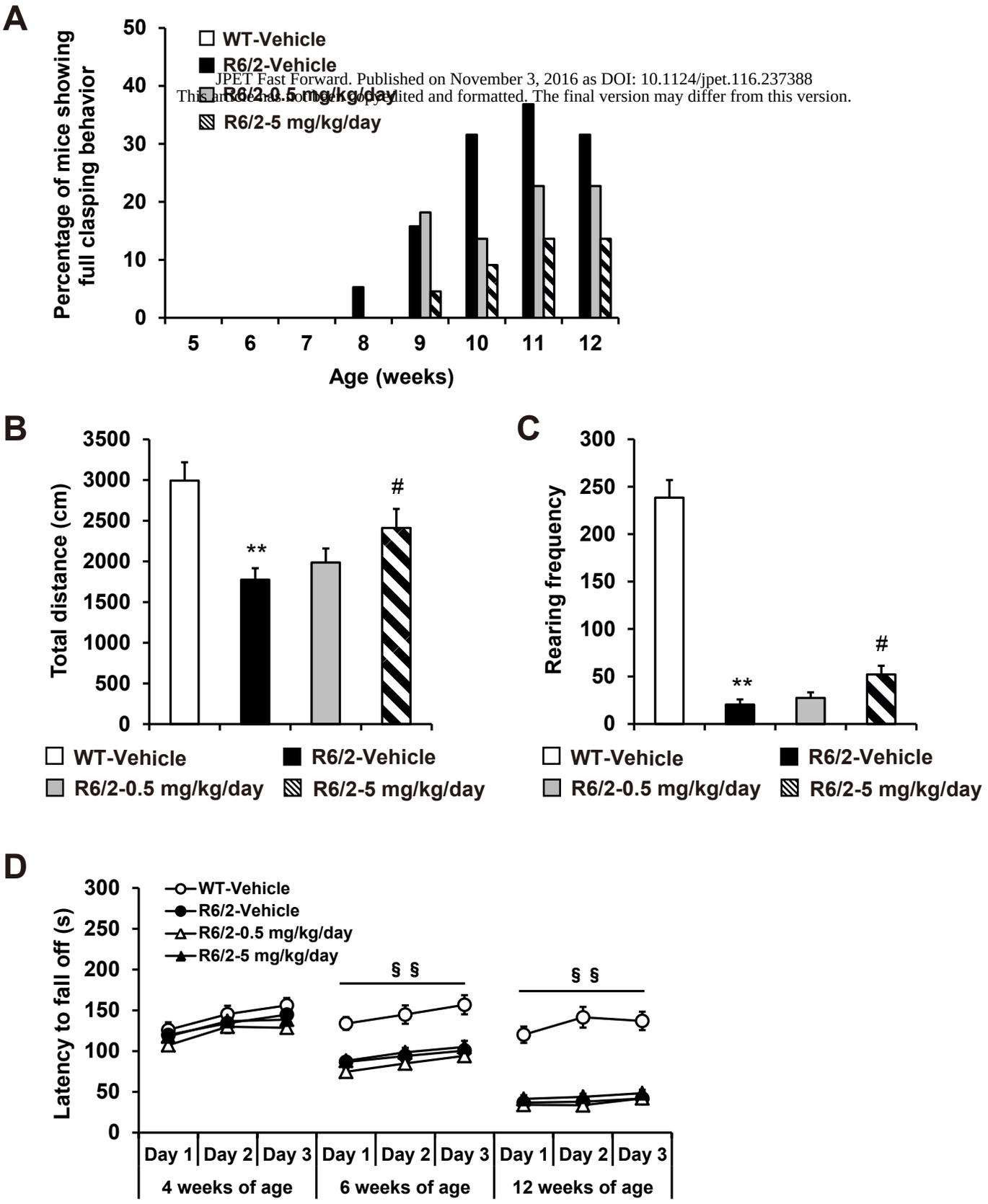

Figure 4

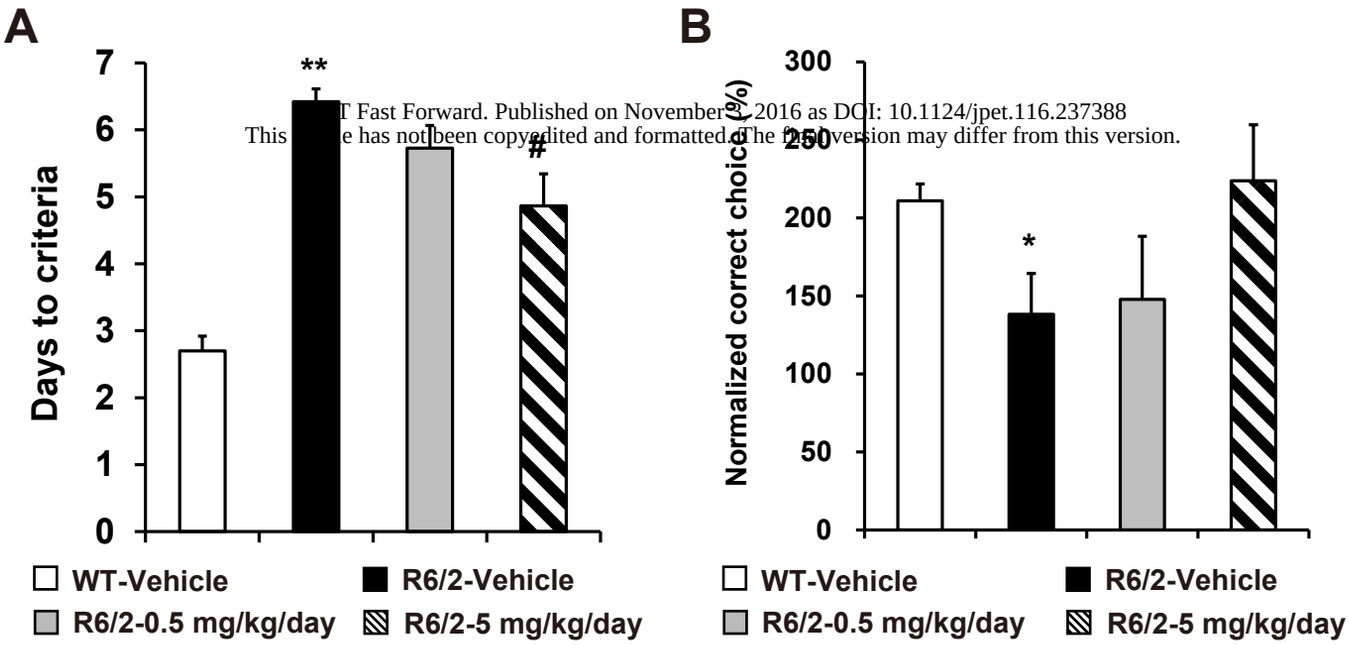

Figure 5

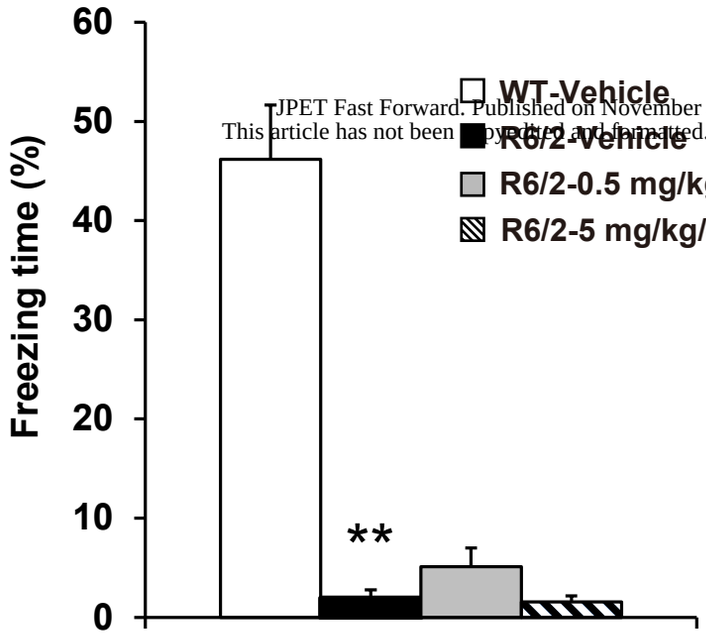

Figure 6